J Mater Sci: Mater Med (2008) 19:877–882
DOI 10.1007/s10856-007-3174-7

STEM-HAADF electron microscopy analysis of the central dark line defect of human tooth enamel crystallites

Jose Reyes Gasga · Georgina Carbajal-de-la-Torre · Etienne Bres · Ivet M. Gil-Chavarria · Ana G. Rodríguez-Hernández · Ramiro Garcia-Garcia

Received: 31 October 2005 / Accepted: 17 May 2007 / Published online: 1 August 2007

Abstract When human tooth enamel is observed with the Transmission Electron Microscope (TEM), a structural defect is registered in the central region of their nanometric grains or crystallites. This defect has been named as Central Dark Line (CDL) and its structure and function in the enamel structure have been unknown yet. In this work we present the TEM analysis to these crystallites using the High Angle Annular Dark Field (HAADF) technique. Our results suggest that the CDL region is the calcium richest part of the human tooth enamel crystallites.

Introduction

Human tooth enamel is composed by 96 wt% of inorganic material, mainly hydroxyapatite (HAP), and 4% of organic material, consisting essentially by two classes of proteins: amelogenins and enamelins. Enamel is formed by prisms in the size range of tenths of microns, which run from the enamel–dentin junction to the enamel surface. These prisms are formed by many elongated-plate-like crystallites whose diameter is from 50 nm to 100 nm wide and from 300 nm to 500 nm long, approximately. The enamel crystallites are observed with the transmission electron microscope (TEM), exhibiting a line of 1–1.5 nm width along their centers [1–6]. This line has been named as “central dark line” (CDL), although its contrast is focusing dependent: it is dark in under-focus, disappears when the image goes through focus, and it is white in over-focus [4], resembling the Fresnel fringes behavior in a phase-contrast image. The observance of this CDL both in plan view (transversal) and along cross-sectioned view (longitudinal) enamel samples indicates that it certainly corresponds to a plane but not to a line. However, “central dark line” has been the name used to identify it.

In order to visualize its structure, the CDL has been attributed to the presence of planar defects such as dislocations and grain boundaries [7–9], to the presence of a layer of octocalcium phosphate (OCP) in dentine crystals [10], and more recently to the presence of a central planar defect which was observed in human tooth enamel crystals using Atomic Force Microscopy [11]. The study of this “line” in the human tooth enamel crystallites is of particular interest because it represents a zone that undergoes preferential dissolution during early stages of the carious process [6, 9, 12, 13]. Therefore the knowledge of its structure, properties and chemical composition is crucial to understand the role that it plays on the enamel structure and, even, to combat and prevent the carious process.

In this work we carried out the structural analysis of the CDL by TEM with the aim of find the differences, if there is one, between the enamel HAP and its CDL. We have used the techniques of high resolution TEM images

J. R. Gasga (✉) · G. Carbajal-de-la-Torre · I. M. Gil-Chavarria · A. G. Rodríguez-Hernández · R. Garcia-Garcia
Instituto de Física, UNAM, Apartado Postal 20-364, 01000 Mexico, DF, Mexico
e-mail: jreyes@fisica.unam.mx

G. Carbajal-de-la-Torre · E. Bres
Laboratorie de Structure et des Proprietes del ÍEtat Solide CNRS UMR 8008, Universite des Scinces et des Technologies de Lille, Batiment C6, 59650 Villenueve d’Ascq, France

I. M. Gil-Chavarria · A. G. Rodríguez-Hernández
Facultad de Odontología, UNAM, Unidad de Posgrado, Circuito de la Investigación Científica, Cd, Universitaria, 04510 Coyoacan, Mexico, DF, Mexico

(HRTEM) and high angle annular dark field (HAADF) images produced in a scanning transmission electron microscope (STEM) unit, which will be referred as STEM-HAADF hereafter. STEM-HAADF is a technique that allows us observing of electron-beam-sensible samples with considerable reduced electron-beam damage, which is very important in the case of enamel where the interaction with the TEM electron beam produces severe structural changes in a short time [5, 6, 9]. We must mention that the analysis with characteristic X-ray by energy dispersive spectroscopy (EDS) in TEM around the CDL has been already carried out [14], but the results on its chemical composition where not as conclusive as in the case reported in this work.

The STEM-HAADF image is formed by detecting the electron flux scattered in angles that are function of the atomic number Z through the Z^2 dependence [15]. Thus, the annular HAADF detector in a STEM produces incoherent images of crystalline materials with strong compositional information [16–19] representing an elemental map (Z-contrast image) which can be quantified using an appropriated cross section [20]. Therefore, the reversal contrasts normally observed in the N-beam phase contrast of HRTEM by thickness and defocus images are not presented in STEM-HAADF images. In the case of enamel, then, the region with brighter contrast in STEM HAADF images will indicate the presence of the heaviest element, i.e. regions with high concentrations of Ca ions ($Z = 20$). Regions with P ($Z = 15$), O ($Z = 8$), and lighter elements will produce a gray contrast.

Experimental procedure

In order to perform the TEM analysis, human tooth enamel was milling in an Agate mortar, calcinated at 200 °C for removing any organic material, and filtered through a 325 mesh grid. The powder was supported on Cu grids that were covered previously with a lacey plastic and carbon films. Afterwards these Cu grids, already with the enamel powder, were re-covered again with a carbon film of 20 nm thick to minimize both electron beam damage and electrical charge effects produced during TEM observation of the enamel grains [6, 9, 12, 21]. A JEOL-FEG-2010-EX microscope was used for HRTEM and STEM-HAADF observations. This microscope is equipped with Schottky-type field emission gun, ultra-high resolution pole piece (Cs = 0.5 mm), and a scanning transmission electron microscope (STEM) unit with high angle annular dark field (HAADF) detector operating at 200 kV. The Digital Micrograph (DM) software from GATAN was used for digital image processing and statistics measurements.

Results

For TEM of the enamel sample in powder all that have to be done is to defocus the image of the enamel crystallite under observation every moment to see the CDL contrast, and the observation has to be so quickly because the electron beam damage [15]. Figure 1 shows the HRTEM images of two the enamel crystallites. It is worth mentioning that the CDL is always observed together with the $[10\bar{1}0]$ fringes, whose periodicity is 0.817 nm.

Figure 2 shows the best HRTEM image obtained for an enamel crystallite with some traces of a CDL (indicated by the arrow). The indexing of the Fast Fourier Transform (FFT) of this image (Fig. 2b), taken with the DM software, indicates that the image is along the $[1\bar{2}10]$ zone axis of the hydroxyapatite unit cell. Using once again the DM software this image can be processed to enhance the CDL contrast, as shown in Fig. 3. However, although these images are very impressive, the analysis of the CDL structure is not simple because the related information is part of the diffuse scattering.

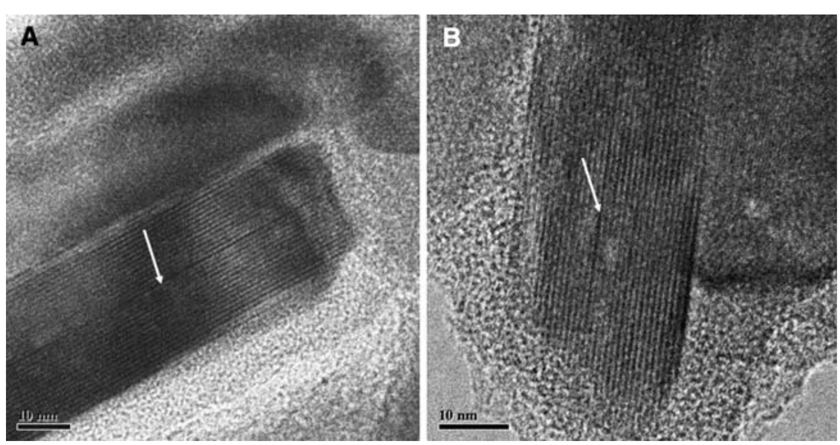

Fig. 1 HRTEM images of two human tooth enamel crystallites. The CDL is indicated by the arrow

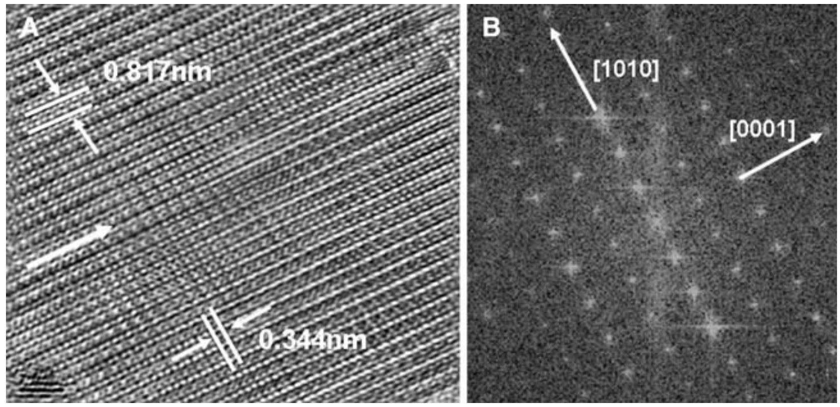

Fig. 2 (**a**) HRTEM image of one of the human tooth enamel crystallite where the CDL (indicated by the arrow) can be observed. (**b**) FFT of the image in (**a**) indicating that the image is along the $[1\bar{2}10]$ zone axis of the HAP unit cell

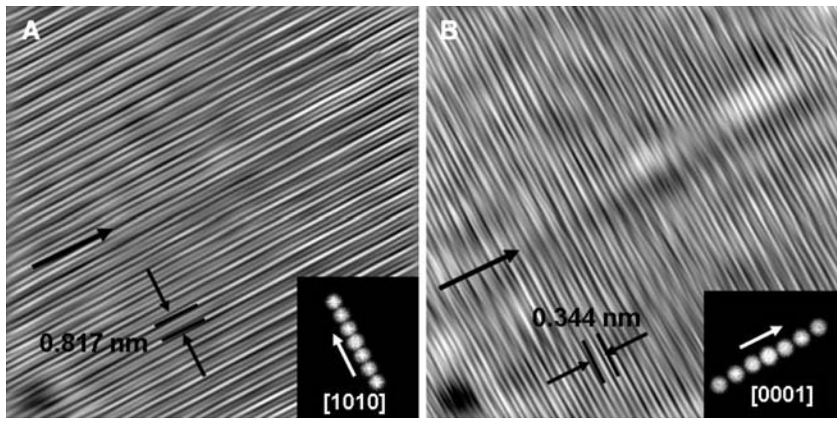

Fig. 3 Images processed from Fig. 2a using the FFT shown in Fig. 2b. The filters used for the processing are shown in the insets. (**a**) $[10\bar{1}0]$ lines, (**b**) [0001] lines. The arrows in the images indicate the CDL positions and in the insets indicate the direction

To get better information on the structure of the CDL, let us analyze the STEM-HAADF images of the enamel crystallites based on their contrast. Figure 4 shows the comparison of the contrast in TEM images and their corresponding STEM-HAADF. Note the reverse in contrast shown in these two types of images, for example the black in TEM image (Fig. 4a) is white in the STEM-HAADF image (Fig. 4b). The whiter zone in the STEM-HAADF image shown in Fig. 4b corresponds to the CDL, which indicates that the structure of the CDL is such that it contains more calcium than the rest of the enamel crystallite. Using the DM software, the image shown in Fig. 4b was processed to enhance its contrast. The results are shown in Fig. 5. In all the cases the contrast for the CDL was the brightest one.

In order to obtain more information from the TEM and STEM-HAADF images of the CDL, we measured the inter-linear periodicity observed in these two types of images (Fig. 6). Note in Fig. 6 that the mean value for this periodicity in the HRTEM images was of 0.877 nm with a standard deviation of 0.071, while in the STEM-HAADF images it was of 0.863 nm with a standard deviation of 0.0298. These values are bigger than the one reported for the $[10\bar{1}0]$ fringes of HAP, which correspond to 0.817 nm. What would be the meaning of this result? The way to obtain a HRTEM image is allowing many reflections through the objective aperture, so the lines observed in this image are produced by an interference process of these reflexions, and although their periodicity is related with the atomic spacing, the meaning for an increment as the one observed in this work is not straightforward. However, in the case of the STEM-HAADF images, the lines represent the periodicity of the atomic rows of Ca. Therefore, it is quite clear that the enamel crystallite shows an increment in its lattice parameter with respect to the HAP unit cell.

Discussion

The STEM-HAADF images show that the CDL is richer in calcium than the rest of the enamel crystallite. It is well known that the inorganic material of the human tooth enamel is mainly composed of HAP, $Ca_{10}(PO_4)_6(OH)_2$, although stoichiometrically speaking, HAP in enamel does not correspond to the previous chemical formulae because many elements such as Mg, Na, and Cl are also included in its unit cell. Thus, a carbonated or deficient HAP, $Ca_5(PO_4,CO_3)_3OH$, was suggested as a better representing compound. Both HAP and carbonated HAP (c-HAP) have a Ca/P ratio of 1.67 [22–24].

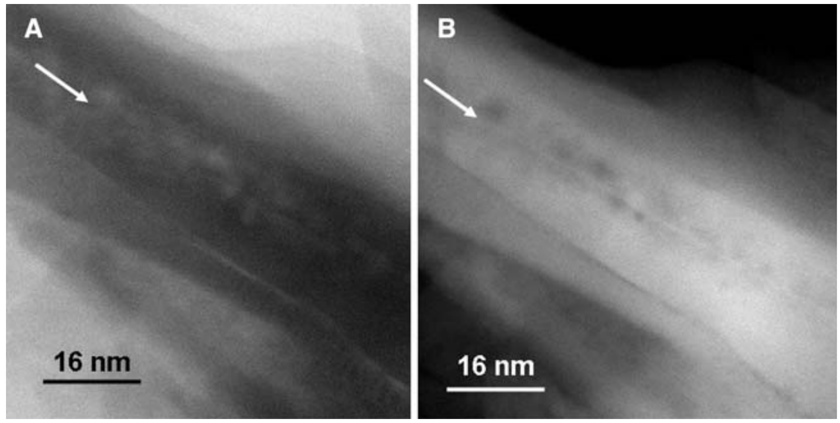

Fig. 4 Comparison between the TEM (**a**) and STEM-HAADF (**b**) images of the same human tooth enamel crystallite. Note the reverse of contrast between them and the contrast shown by the CDL

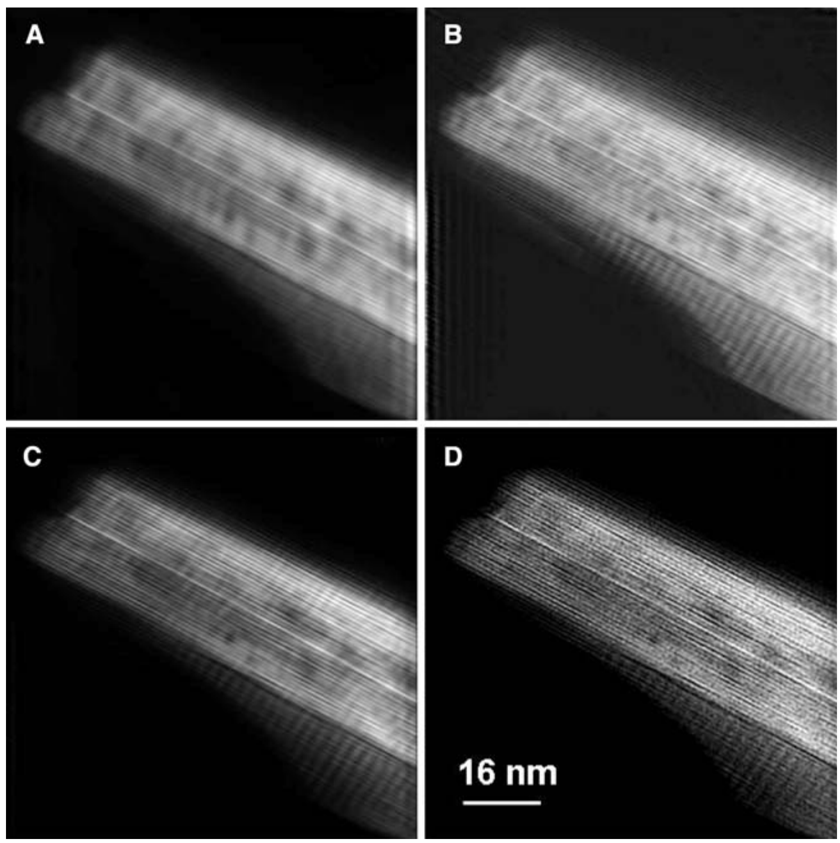

Fig. 5 Four processed images from the STEM-HAADF image shown in figure 4b to enhance its contrast. Note that in all the cases the contrast of the CDL is the brightest one.

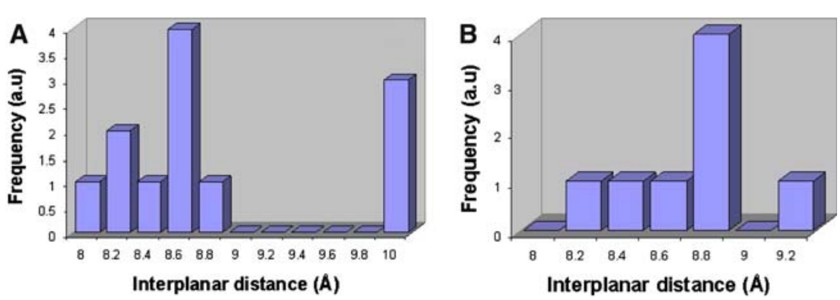

Fig. 6 Frequency distribution of the inter-linear periodicity observed both in the HRTEM images (**a**) and the STEM-HAADF images (**b**) where the CDL was observed. For HRTEM images the mean value was 0.877 nm with a standard deviation of 0.071. For STEM-HAADF images, the mean value was 0.863 nm with a standard deviation of 0.0298

Based on some experimental results that indicated that HAP is able to growth in an epitaxial way on the surface of OCP [25, 26], it has been suggested that the CDL observed in the nanometric-sized grains of human tooth enamel corresponds to the growth of HAP on a one unit-cell- thick layer of OCP [27–30]. A CDĹs model such as this would fit quite well with the HRTEM observations. Structurally speaking there are some similarities between the unit cells of HAP (hexagonal P6_3/m, a = 9.418, c = 6.884 A) and OCP, whose chemical formulae is $Ca_8H_2(PO_4)_6(H_2O)_5$ (triclinic P1, a = 19.87, b = 9.63, c = 6.87 A; α = 90.13°, β = 92.13°, γ = 108.36°), so it is not difficult to suggest how an HAP–OCP interface can be built [28, 29]. However, a CDL structure related with OCP does not agree quite well with the results that presented in this work. The Ca/P ratio in OCP is 1.33; i.e. it has less calcium than in HAP, where it is of 1.67. The concentration of atoms of Ca in the OCP (~4.09 Ca atoms/nm^3) is also much lower than in HAP (~18.86 Ca atoms/nm^3). This also excludes the presence of an OCP layer as reported by Bodier-Houllé et al. [10] in developing dentine.

One possible explanation for our results could be the existence of a structural defect located at the CDL at which an increase of Ca concentration is observed. Fernández et al. [29] have already proposed the existence of structural defect in the HAP–OCP interface. An X-ray topography investigation of natural apatite [31] have shown the presence of grain boundaries and a large density of dislocations with probable Burgers vectors $\mathbf{b} = a[11\bar{2}0]$ and $\mathbf{b} = c[0001]$. On the other hand, HRTEM studies on human tooth enamel crystals [9] have shown the existence of two types of planar defects: (1) a twin boundary parallel to the $(1\bar{1}00)$ plane, and (2) a low angle grain boundary with an angle of 1.74° between $(1\bar{1}00)$ planes on the two sides of the crystals. Such these two defects are consistent with the contrast of the CDL, additional that CDL type-like contrast has been also observed in dislocations of grain boundaries of NiO [32]. All this, together with our results, confirm the fact that CDL type contrast could be observed in crystals without OCP layers or with OCP layers with Ca-rich defect at the interface. However the relationship between an OCP layer and the presence of defects still remains as an open question. Are these Ca-rich defects really formed during the transformation of OCP into HAP?

Conclusion

STEM-HAADF images presented in this work indicated a rich concentration of Ca around the CDL region. This is a strongly experimental support against the model which would like to interpret the CDL observance as an effect associated to a OCP planar structure surrender by the environment of HAP since the Ca/P ratio is bigger in HAP (1.67) than in OCP (1.33). Moreover, the results here presented indicate the possible existence of structural defects rich in Ca at the zone of the CDL, which opens the possibility of existence of a HAP–OCP interface with a high density of Ca-rich structural defects.

Acknowledgements We acknowledge to L. Rendón, C. Magaña, R. Hernández, J. Cañetas, S. Tehuacanero, P. Mexía, and M. Aguilar for their technical help. We thank the Laboratorio Central de Microscopy of the IFUNAM for electron microscopy facilities. We also acknowledge the economical support from DGAPA-UNAM under the project IN-117906.

References

1. E. RÖNNHOLM, *J. Ultrastruct. Res.* **6** (1962) 249
2. M. U. NYLEN, E. D. EANES and K. A. OMNELL, *J. Cell. Biol.* **18** (1963) 109
3. A. F. MARSHALL and K. R. LAWLESS, *J. Dent. Res.* **60** (1981) 1773
4. D. G. A. NELSON, G. J. WOOD, J. C. BARRY and J. D. B. FEATHERSTONE, *Ultramicroscopy* **19** (1986) 253
5. E. F. BRES, W. G. WADDINGTON, J. C. VOEGEL, J. C. BARRY and R. M. FRANK, *Biophysics* **1** (1986) 1105
6. T. YANAGISAWA and Y. MIAKE, *J. Electron Microsc.* **52** (2003) 605
7. E. F. BRÈS, J. L. HUTCHISON, J.-C. VOEGEL and R. M. FRANK, *Journal de Physique* **51** (1990) C1-97
8. E. F. BRÈS, W. G. WADDINGTON, J.-C. VOEGEL, J. C. BARRY and R. M. FRANK, *Biophys. J.* **50** (1986) 1185
9. E. F. BRÈS, J. C. BARRY and J. L. HUTCHISON, *Ultramicroscopy* **12** (1984) 367
10. P. BODIER-HOULLÉ, P. STEUER, J.-C. VOEGEL and F. J. G. CUISINIER, *Acta Cryst.* **D54** (1998) 1377
11. C. ROBINSON, S. CONNELL, J. KIRKHAM, R. SHORE and A. SMITH, *J. Mater. Chem.* **14** (2004) 2242
12. D. B. SCOTT, J. W. SIMMELINK and V. NYGAARD, *J. Dent. Res.* **53** (1974) 165
13. J.-C. VOEGEL and R. M. FRANK, *Calcif. Tissue Res.* **24** (1997) 19
14. A. BELIO-REYES, L. VARGAS-ULLOA, L. F. JIMENEZ-GARCIA and J. REYES-GASGA, *Latin-Am. J. Metallurgy Mater.* **19** (1999) 52
15. M. S. ISAACSON, M. OHTSUKI and M. UTLAUT, in "Introduction to the Analytical Electron Microscopy", edited by J. J. HREN, J. I. GOLDSTEIN and D. C. JOY (Plenum Press, New York, 1979) p. 343
16. V. CREWE, J. P. LANGMORE and M. S. ISAACSON, in "Physical Aspects of Electron Microscopy and Microbeam Analysis", edited by B. M. SIEGEL and D. R. BEMAN (Wiley, New York, 1975) p. 47
17. A. Howie, *J. Microsc.* **117** (1979) 11
18. J. M. COWLEY, *Ultramicroscopy* **2** (1976) 258
19. S. J. PENNYCOOK, S. D. BERGER and R. J. CULBERTSON, *J. Microsc.* **144** (1986) 229
20. S. J. PENNYCOOK and D. E. JESSON, *Ultramicroscopy* **37** (1991) 14
21. J. REYES-GASGA and R. GARCIA-GARCIA, *Radiat. Phys. Chem.* **64** (2002) 359
22. L. F. LOZANO, M. A. PEÑA-RICO, A. HEREDIA, J. OCOTLAN-FLORES, A. GOMEZ-CORTES, R. VELÁSQUEZ, I. A. BELIO and L. BUCIO, *J. Mater. Sci.* **38** (2003) 4777

23. C. P. LIN, B. S. LEE, S. H. KOK, W. H. LAN, Y. C. TSENG and F. H. LIN, *J. Mat. Sci.* **11** (2000) 373
24. F. H. LIN, C. J. LIAO, K. S. CHEN and J. S. SUN, *Biomaterials* **19** (1998) 1101
25. M. IIJIMA, H. THODA and Y. MORIWAKI, *J. Cryst. Growth* **116** (1992) 319
26. M. IIJIMA and Y. MORIWAKI, *J. Cryst. Growth* **194** (1998) 125; *J. Cryst. Growth* **198–199** (1999) 670
27. Y. MIAKE, S. SHIMODA, M. FUKAE and T. AOBA, *Calcif. Tissue Int.* **53** (1993) 249
28. A. G. RODRIGUEZ-HERNANDEZ, M. E. FERNANDEZ, G. CARBAJAL DE LA TORRE, R. GARCIA-GARCIA and J. REYES-GASGA, in “Electron Microscopy of Molecular and Atom-Scale Mechanical Behavior, Chemistry and Structure”, edited by D. C. MARTIN, D. A. MULLER, P. A. MIDGLEY and E. A. STACH, *Mater. Res. Soc. Symp. Proc.* **839** (2005), P6.10.1
29. M. E. FERNÁNDEZ, J. A. ASCENCIO, C. ZORRILLA-CANGAS, R. GARCÍA-GARCÍA and J. REYES-GASGA, *Acta Cryst. B* **59** (2003) 175
30. G. H. NANCOLLAS, *Pure Appl. Chem.* **64** (1992) 1673
31. P. P. PHAKEY and J. R. LEONARD, *J. Appl. Cryst.* **3** (1970) 38
32. M. RÜHLE and S. L. SASS, *Philos. Mag. A* **49** (1984) 759